

IMPROVING HYDROCYCLONE EFFICIENCY BY CHANGING GEOMETRIC PARAMETERS

Zsolt Hegyes 

MSc student, Institute of Energy Engineering and Chemical Machinery, University of Miskolc
3515 Miskolc, Miskolc-Egyetemváros, e-mail: hegyes.zs97@gmail.com

Máté Petrik 

assistant professor, Institute of Energy Engineering and Chemical Machinery, University of Miskolc
3515 Miskolc, Miskolc-Egyetemváros, e-mail: mate.petrik@uni-miskolc.hu

Gábor L. Szepesi 

associate professor, Institute of Energy Engineering and Chemical Machinery, University of Miskolc
3515 Miskolc, Miskolc-Egyetemváros, e-mail: gabor.szepesi@uni-miskolc.hu

Abstract

Hydrocyclone is a very simple and cost-effective way to separate inhomogeneous fluid-solid mixtures. It is important to ensure adequate separation efficiency during their operation. Many researchers have worked to identify the factors that influence separation. Geometry has been identified as one of the most important influencing factors. This article summarises the results of this research in order to provide a comprehensive picture of the importance and impact of each geometric element.

Keywords: hydrocyclone, geometric parameters, optimization possibilities

1. Introduction

Many industrial sectors, such as mining or the oil industry, require equipment to separate immiscible suspensions and emulsions. The hydrocyclone is one of the perfect tool for this purpose. Its simple design, together with the fact that it has no moving parts, makes it a very cost-effective operation. A general hydrocyclone design is shown in Figure 1.

The separation is based on centrifugal principles. The solid-liquid mixture entering the inlet pipe spirals down the cyclone wall under gravitational and centrifugal forces. The heavier phase exits along the wall through the lower outlet pipe (hereafter referred to as spigot), while the lighter phase leaves the hydrocyclone through the vortex finder in a secondary vortex. An important parameter during the separation process is the efficiency of the material to be separated, which can be determined from the ratio of the fluid density measured in the two outlet pipes. The separation efficiency is influenced by several factors such as density, particle size, geometry, etc. In the following the Authors give a brief overview of the results of research on geometry optimization.

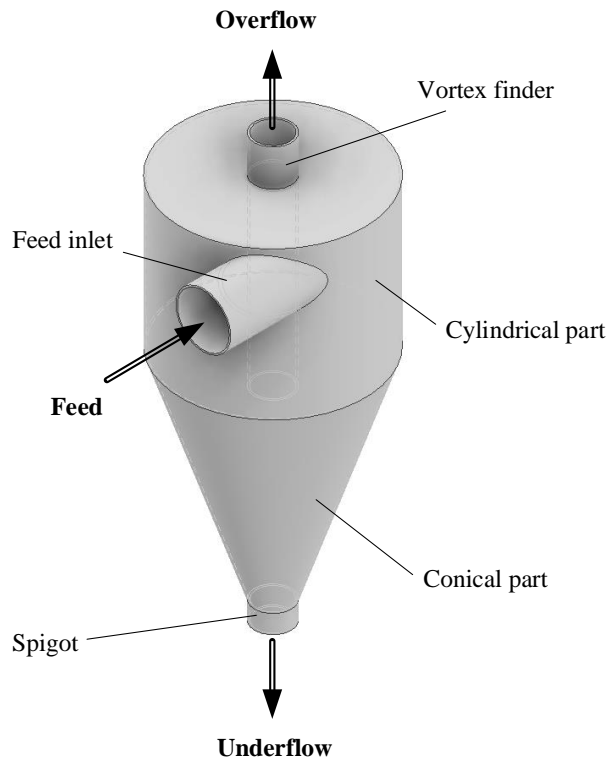


Figure 1. A typical hydrocyclone structure

2. Vortex finder

Observations on the optimization of the vortex finder geometry are shown in Figure 2. In the figure, the geometry marked a) corresponds to the initial geometry. Research has shown that a certain increase in efficiency can be achieved by modifying the vortex tracker tube alone, but this is not the most influential geometry (Zhao et al., 2019).

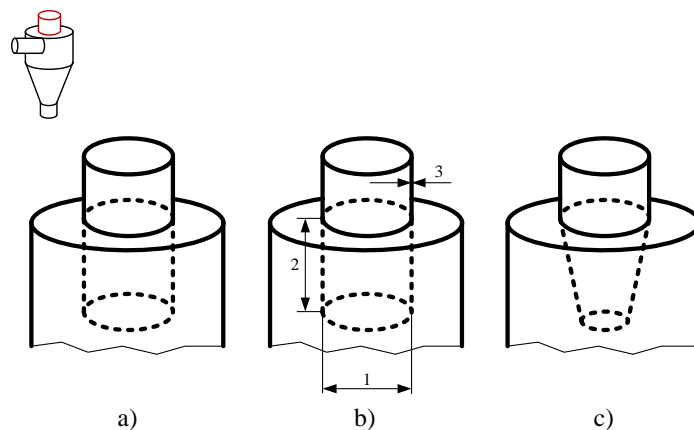


Figure 2. Different types of vortex finders

Figure 2 (b) shows the variation of three parameters that have been studied by several researchers (Zhao et al., 2019; Young et al., 1994; Statie et al., 2001; Delgadillo and Rajamani, 2007). The general conclusion on the length of the vortex finder is that increasing the length is beneficial for the separation (Statie et al., 2001; Delgadillo and Rajamani, 2007). Most importantly, the lower part of the vortex finder tube should extend beyond the inlet of the feed stub to avoid possible backflows (Statie et al., 2001). Further increases in the length of the vortex finder tube do not cause significant changes. Increasing the diameter will increase the amount of heavier phase carried away in the vortex finder tube.

In some cases, it is sufficient to specify a minimum diameter (for example in case the cleanup of oily water) (Young et al., 1994; Statie et al., 2001). It is also important to keep in mind that with increased diameter, the pressure drop is reduced, which has a negative effect on separation. Increasing the *wall thickness* in this case means increasing the outer diameter of the vortex detector tube. Increasing the wall thickness decreases the tangential velocity and the pressure drop, but some backflow phenomena can be eliminated by an optimal choice. Increasing the wall thickness has little influence on the separation (Zhao et al., 2019). Experiments have also been carried out on the design shown in Figure 2 (c) part. The results concluded that it is not practical to deviate from the design shown in Figure 2 (a) (Chu et al., 2000).

3. Upper shell part

The upper shell part is responsible for the formation of a stable vortex and also has a significant influence on the residence time. The basic upper shell part shown on Figure 3/a). Increasing the length of the upper cylindrical part has no significant effect on separation (see Figure 3/ b)). This part is responsible for the formation of a stable vortex during hydrocyclone operation. A shorter cylindrical section can provide better separation by reducing the kinetic energy lost by the outgoing fluid (Young et al., 1994; Statie et al., 2001; Chu et al., 2000; Bradley, 1965). However, increasing the diameter already has a significant effect on separation. Here it is important to specify the correct diameter, as using a too small diameter leads to poor separation, but using too large a diameter can cause fluctuations, which have a negative impact on cyclone efficiency (Statie et al., 2001).

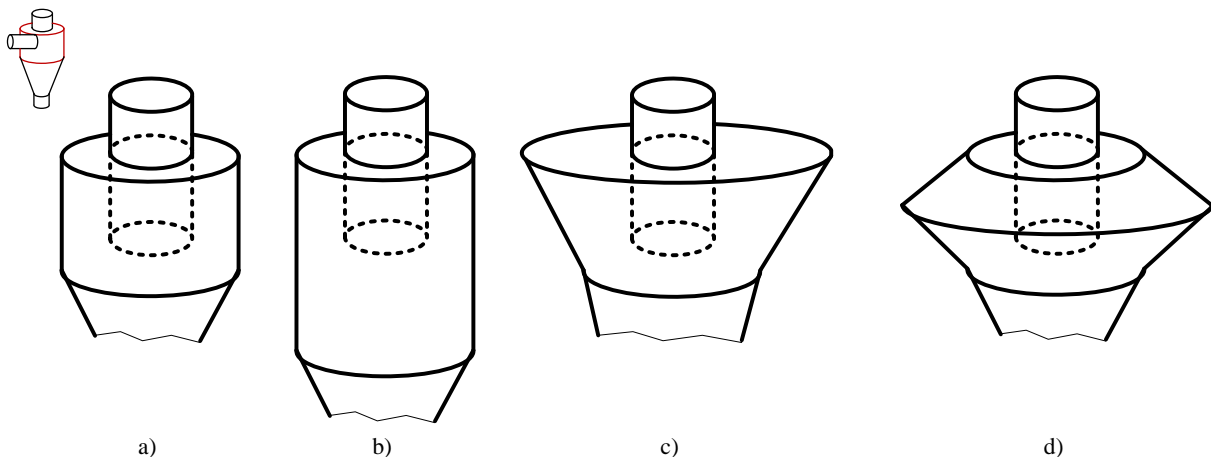


Figure 3. Different types of upper shell part

The application of Figure 3 variations c) and d) did not lead to an improvement in efficiency and are therefore not justified (Delgadillo and Rajamani, 2007).

4. Feed inlet nozzle

This part of the hydrocyclone has the greatest influence on the efficiency of the separation. Several modifications have been developed by the researchers and these are shown in Figure 4. Research on the loading stub can be divided into 2 major parts. One part is related to the way of connection and the other part is related to the cross section of the inlet nozzle. The hydrocyclone geometry used by Rietema (Rietema, 1961a, 1961b) was used in this research.

4.1. Research and results according to the configurations of the inlet nozzle

Research on the inlet nozzle configurations has led to a deviation from the tangential entry, which was achieved by introducing the stub at different angles (Chu et al., 2000). However, these did not lead to good results and the tangential entry was retained (see on Figure 4/a)). Several modifications to the tangential entry have been made and are summarised in Figure 4.

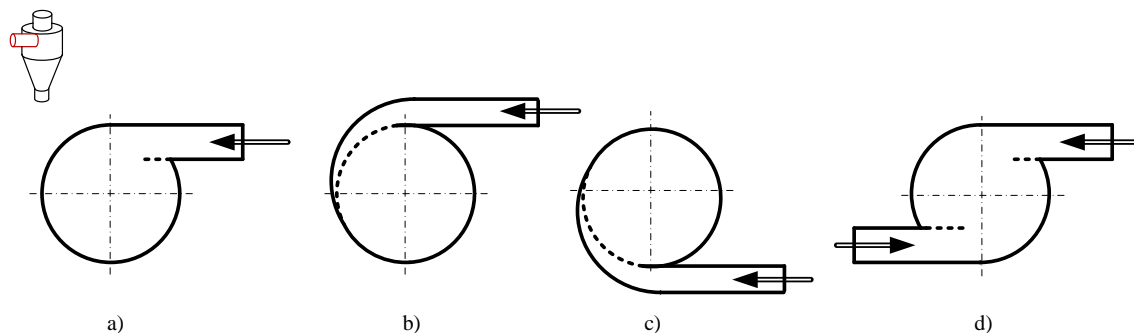


Figure 4. Feed inlet configurations (Rietema, 1961a)

In Figure 4 d), double introduction has been shown to achieve a more efficient separation than single introduction (a) part) (Aldrich, 2015). Figure 4 b) and c) show an involute and involute ramp introduction. This type of introduction has been studied in detail by Li et al. 2020. The researchers concluded that the curved input has a beneficial effect on the decoupling. The modification increased the tangential velocity and reduced the formation of harmful backflows. A further effect of the curved inlet is an increase in residence time, which has an additional beneficial effect on separation. However, it is important to bear in mind that such a design is often complex and expensive.

4.2. Research and results according to the cross section of the inlet nozzle

The hydrocyclone geometry used by Rietema (Rietema, 1961a, 1961b) was also used as a basis for the study of the cross-section of the feeding nozzle. It was still circular in cross-section, however, several studies have shown that an angular cross-section is better (Rocha et al. 2020; Tang et al., 2017). Figure 5 shows the hydrocyclone geometries used by C.A.O. Rocha et al. 2020. Here, it is concluded that each of the loading stub geometries was found to be superior to the cyclone a). However, the best cross section was found to be the 7x7 cross section (which means the edge length of the cross section of the feed

nozzle in mm) (b), as it had the best efficiency and the highest tangential velocity at the same loading velocities.

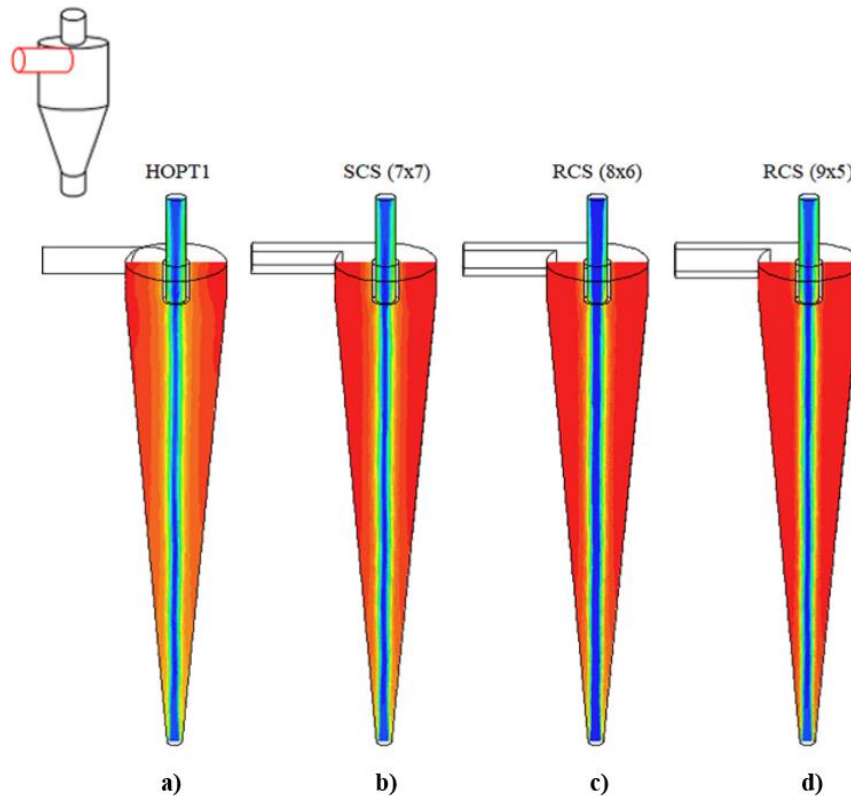


Figure 5. Different sizes of inlet cross sections (Tang et al., 2017)

4.3. Sizing and checking of an industrial-sized hydrocyclone inlet nozzle

In the section 4, the different inlet nozzle variations for hydrocyclones were described, together with their advantages and disadvantages. The hydrocyclones described are all small cyclones (average diameter of 75 mm), which are not relevant from the point of view of silica sizing, as they are very oversized for their size. For industrial-sized hydrocyclones, the stress conditions in the cross-sections loaded with traces must be considered, as the average size of these cyclones can be 300-500 mm in diameter. Since research has shown that an angular cross-section is preferable to a circular inlet (Rocha et al., 2020), the use of an angular inlets would be justified for industrial-sized hydrocyclones. However, that at the junction of a cylindrical shell plus a square coupling, under pressure load, significant stresses can occur in the vicinity of the coupling.

To investigate this problem, the sizing and verification of an industrial-sized ($D=323,9$ mm) hydrocyclone feed inlet is described. The hydrocyclone used for the sizing has the geometry shown in Figure 6, the values of which are given in Table 1. The sizing assumes of a working pressure of 8 bar, the cyclone is made of carbon steel (cylinder part made of P235GH seamless tubes, feed section made of P295GH plate material). The wall thickness of the upper cylinder is 7,1 mm (standard DN 300, type 1), the wall thickness of the feed section is 6 mm. Sizing and checks are carried out in the context of the

standard MSZ EN 13445-3. For sizing and verification, 2 cases are considered. First the connection of the stub using the area comparison method was checked, after the compliance of the nozzle with the inlet pressure load for square vessels according to the standard was also investigated.

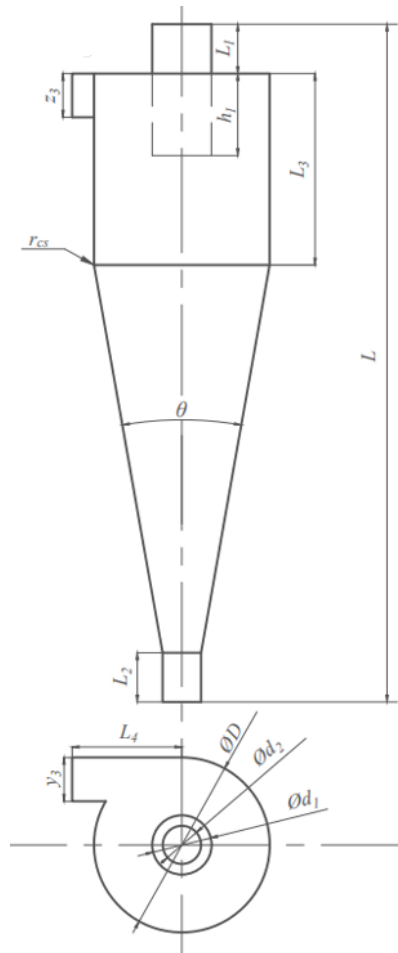


Figure 6. Geometry of the industrial hydrocyclone

Table 1. Hydrocyclone dimensions in mm

Geometry dimensions in mm											
L_1	L_2	L_3	L_4	h_1	D	z_3	y_3	d_1	d_2	r_{cs}	θ
120	100	350	200	150	323.9	80	80	114.3	88.9	20	20

In the area comparison procedure for strength analysis, checking in two views carried out. One is the oblique view and the other is the transverse view, which correspond to the main view and the X-X sectional view in Figure 7. The same area comparison procedure is applied for both views. The procedure is used to determine the load and load bearing cross sections. After the determination, a stub

to be load-bearing if the load force is less than the maximum load capacity of the cross sections was considered. The following equations were used:

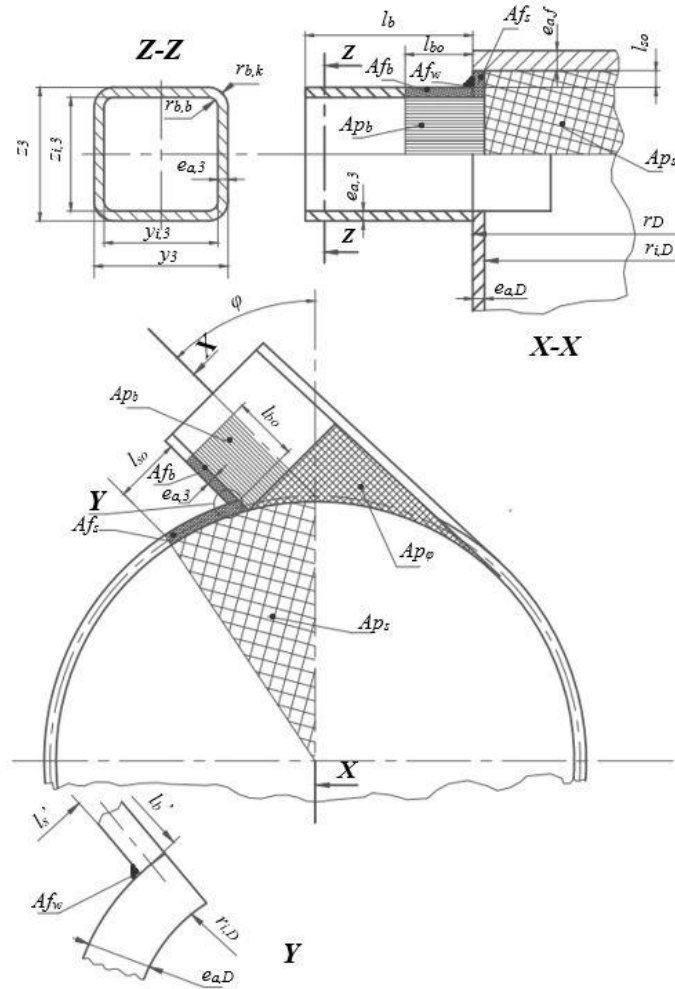


Figure 7. Oblique and transverse view to determine the cross section areas

Stress loaded force:

$$PA_f = (A_{f_s} + A_{f_w}) \cdot (f_{a,D} + 0,5 \cdot P) + A_{f_b} \cdot (f_{ob} - 0,5 \cdot P) \quad (4.1)$$

Pressure loaded force:

$$PA_p = P \cdot (A_{p_s} + A_{p_b} + 0,5 \cdot A_{p_\varphi}) \quad (4.2)$$

Compliance:

$$PA_f \geq PA_p \quad (4.3)$$

The calculations showed a utilization of 28,90% for the cross-section in the main view and 33,01% for the cross-section in the X-X section, which indicated that a visceral stump connection was appropriate.

Another way of checking is to check the internal compressive load of the nozzle made up of flat plates. The check is carried out according to the correlation of the standard MSZ EN 13445-3, where bending and diaphragm stress values are calculated in 5 ranges (see Figure 8).

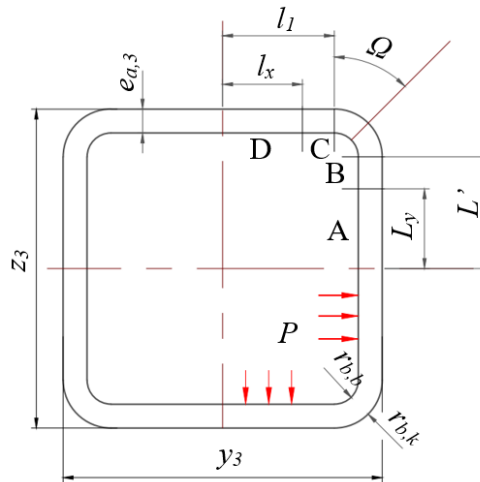


Figure 8. Inlet design for inlet pressure

The determinations gave membrane stress values between 7-10 MPa, well below the specified allowable stress of 191,67 MPa. For the bending stresses, higher values were obtained, which are summarized in Table 2:

Table 2. Bending stress values at design condition

Name	Sign	Value	Dimension
Second moment of area	I_1	4,22	mm ³
Bending stress in Point C	$(\sigma_b)_C$	137,44	MPa
Bending stress in Point D	$(\sigma_b)_D$	-137,44	MPa
Bending stress in Point A	$(\sigma_b)_B$	0	MPa
Bending stress in Point B	$(\sigma_b)_A$	137,44	MPa
Bending stress in Point B-C	$(\sigma_b)_{B-C}$	161,84	MPa

From the values in Table 2, the highest stress is at the B-C corner (along the edge), but even this value does not exceed the allowed stress of 191.67 MPa.

5. Lower conical part

Different cone variations are shown in Figure 9. The conical part is closely related to the residence time. By increasing the residence time, a sharper separation can be achieved, but it is important to bear in

mind that with increased residence time the energy level of the fluid decreases significantly. The reduced energy level carries with it the risk of fluctuation, which has a negative effect on separation. It is important to keep in mind that the cone angle modification shown in Figure 9(b) involves a change in the diameter of the lower outlet stub as well as the upper cylindrical section. To prevent this from occurring, the length of the tapered section must be increased or decreased. Increasing the length will in turn affect the dwell time. It is therefore important to determine the optimum taper angle.

Through a series of experiments, the researchers have identified several ideal cone angles. In general, the cone angle values ranged from 9° to 20° . The exact cone angle ranges determined by each research are shown in Table 3. It is also possible that the taper is omitted completely. An example design shown in Figure 9(c). The usual cyclonic flow pattern can also develop here, and recorded cases in the literature where such a design has resulted in sharper separation (Young et al., 2019; Statie et al., 2001; Chu et al., 2000; Rietema, 1961a).

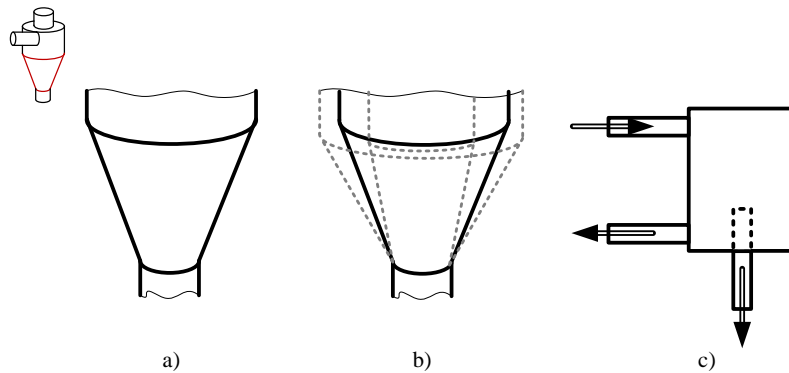


Figure 9. Different types of the conical part

6. Spigot

The geometric modifications applied to the lower outlet spigot are shown in Figure 10. Changing the length of the bottom outlet (spigot) has no significant effect on the separation efficiency but plays an important role in the ideal thickening slurry discharge (Young et al., 2019). Changing the length of the bottom outlet stub has no significant effect on the separation efficiency, in some cases it is completely omitted, and the thickening slurry is discharged directly into a collection tank (Bradley, 1965).

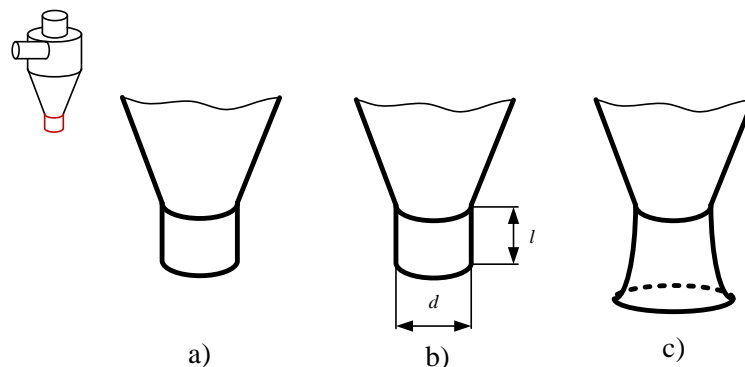


Figure 10. Different types of spigots

7. Summary

Research has shown that finding the optimal hydrocyclone geometry is not a simple task. The most important geometrical parameter is the inlet nozzle and the main diameter of the cyclone, but each geometrical parameter is involved in the development of the right flow conditions. Accordingly, the researchers established geometric ratios, which are illustrated in Table 3. By adhering to these ratios, optimum operating conditions can be achieved.

Table 3. Operating variables on performance (Aldrich, 2015)

Researcher	d_3/D	d_2/D	L/D	h/D	β
Bradley	0,133-0.143	0,200	6,850	0,333	9°
Krebs	0,267	0,159	5,874	-	12,7°
Rietema	0,280	0,340	5	0,400	15-20°

8. Nomenclature

Latin letters

A_{fb}	stress loaded cross-sectional area of the nozzle	[mm ²]
A_{fs}	stress loaded cross-sectional area of the shell	[mm ²]
A_{pb}	pressure loaded cross-sectional area of the nozzle	[mm ²]
A_{ps}	pressure loaded cross-sectional area of the shell	[mm ²]
$A_{p\varphi}$	additional pressure loaded cross-sectional area of the nozzle	[mm ²]
d_2	diameter of the spigot	[mm]
d_3	diameter of the feed inlet	[mm]
D	main diameter of the cyclone	[mm]
$f_{d,D}$	allowable stress of upper cylindrical part	[MPa]
f_{ob}	allowable stress of the nozzle	[MPa]
L	total length of the cyclone	[mm]
h	length of the vortex finder inside of the cyclone	[mm]
P	design pressure	[bar]
PA_f	pressure loaded force	[N]
PA_p	stress loaded force	[N]

Greek letters

β	angle of the conical part	[°]
φ	angle of the nozzle	[°]

References

- [1] Zhao, Q., Cui, B., Wei, D., Song, T., and Feng, Y. (2019). Numerical analysis of the flow field and separation performance in hydrocyclones with different vortex finder wall thickness. *Powder Technology*, 345, 478-491. <https://doi.org/10.1016/j.powtec.2019.01.030>
- [2] Young, G. A. B., Wakley, W. D., Taggart, D. L., Andrews, S. L., and Worrell, J. R. (1994). *Oil-water separation using hydrocyclones: An experimental search for optimum dimensions*. [https://doi.org/10.1016/0920-4105\(94\)90061-2](https://doi.org/10.1016/0920-4105(94)90061-2)

- [3] Stăte, E. C., Salcudean, M. E., and Gartshore, L. S.: The Influence of Hydrocyclone Geometry on Separation and Fibre Classification.
- [4] Delgadillo, J. A., and Rajamani, R. K. (2007). Exploration of hydrocyclone designs using computational fluid dynamics. *International Journal of Mineral Processing*, 84(1-4), 252-261, <https://doi.org/10.1016/j.minpro.2006.07.014>
- [5] Chu, L.-Y., Chen, W.-M., and Lee, X.-Z. (2000). *Effect of structural modification on hydrocyclone performance*. Available: www.elsevier.com/locate/seppur
[https://doi.org/10.1016/S1383-5866\(00\)00192-1](https://doi.org/10.1016/S1383-5866(00)00192-1)
- [6] Bradley, D. (1965). *The Hydrocyclone*. International Series of Monographs in Chemical Engineering, Jan. 1965.
- [7] Rietema, K. (1961a). Performance and design of hydrocyclones-III Separating power of the hydrocyclone, *Chemical Engineering Science*, 15, 310-319. [https://doi.org/10.1016/0009-2509\(61\)85035-5](https://doi.org/10.1016/0009-2509(61)85035-5)
- [8] Rietema, K. (1961b). Performance and design of hydrocyclones-IV Design of hydrocyclones. *Chemical Engineering Science*, 15, 320-325. [https://doi.org/10.1016/0009-2509\(61\)85036-7](https://doi.org/10.1016/0009-2509(61)85036-7)
- [9] Aldrich, C. (2015). Hydrocyclones. In *Progress in Filtration and Separation* (pp. 1-24). Elsevier Ltd. <https://doi.org/10.1016/B978-0-12-384746-1.00001-X>
- [10] Rocha, C. A. O., Ullmann, G., Silva, D. O., and Vieira, L. G. M. (2020). Effect of changes in the feed duct on hydrocyclone performance. *Powder Technology*, 374, 283-289. <https://doi.org/10.1016/j.powtec.2020.07.001>
- [11] Tang, B., Xu, Y.-x., Song X.-f., Sun, Z., and Yu, J.-g. (2017). Effect of inlet configuration on hydrocyclone performance. *Transactions of Nonferrous Metals Society of China* (English Edition), 27(7), 1645-1655. [https://doi.org/10.1016/S1003-6326\(17\)60187-0](https://doi.org/10.1016/S1003-6326(17)60187-0)